Realistic Floating Breakwater Design Based on an Optimized 2D Model.

Faisal Mahmuddin [*1], Abdul Latief Had [1,] and Syerly Klara [1]

1. Department of Naval Architecture, Faculty of Engineering, Hasanuddin University, Makassar 91211, Indonesia

Abstract: From previous study, a 2D floating breakwater model which has optimal performance, had been obtained. The performance of the model was verified with numerical relations and an experiment in towing tank as well. Moreover, its performance and characteristics in 3D case were also evaluated in the subsequent study However, because the 3D model is formed by simply extruding the 2D shape in longitudinal direction, it only produces a model with uniform transverse shape which is considered to be less effective and efficient in terms of technical and economical points of view. Consequently, it is needed to modify the model to obtain a more realistic and efficient design without reducing significantly the performance obtained previously. In the present study, several modifications of the original 3D model are performed. The performance and characteristics of the modified models in terms of wave elevations on the free surface are evaluated at various wavelengths by using higher order boundary element method (HOBEM). The accuracy of the computed results is confirmed with Haskind-Newman and energy conservation relations. From the modifications and evaluations of the original model, the effect of modifications to the performance can be realized which could be used to design a more realistic and efficient model.

Key words: Floating breakwater, performance optimization, shape modification, HOBEM, realistic model, wave elevation.

1. Introduction

Since a long time ago, near-shore area has become an important place for people activities. Therefore, it is necessary to protect it from wave attack and other harsh environment conditions. This would enable people to conduct activities in this area conveniently which could also increases their productivity and economic growth around the area.

There are several methods of protection which could be used. One of these methods is to install a floating-type breakwater. This type of floating breakwater has several advantages such as low construction cost, installation flexibility, fresh water preservation, easy repair, etc.

Some of the important matters to consider when choosing a floating breakwater model to be installed are its performance and construction cost. Consequently, less volume models are more preferable since it will be cheaper for construction. Therefore it is important to obtain a model which has less volume without reducing significantly its performance. Moreover, from technical point of view, less material model tends to be lighter. Being lighter is also one of the desirable properties of a floating breakwater.

In this study, an optimized floating breakwater model determined in the previous study by Kashiwagi and Faisal in [1], is modified to obtain a more realistic and efficient floating breakwater model in terms of model volume. It is common that a model with less volume relatively will use less material and weight in constructing the real model.

The original model which will be modified was constructed by extruding an optimized 2D shape obtained from a study by Mahmuddin and Kashiwagi in [2] into horizontal direction. Consequently, the model

has uniform transverse shape which can be considered to be less effective and efficient. Therefore, it is needed to modify this shape to obtain a more realistic and efficient model without reducing significantly the performance obtained previously.

In order to analyze the performance of the modified models, higher order boundary element method (HOBEM) is employed. HOBEM which is based on the potential flow theory divides the body into certain number of panels and represents both quadrilateral panels and unknown velocity potentials with quadratic representation. The hydrodynamic forces, body motions and wave elevation on the free surface around the body can be computed and analyzed with this method.

The accuracy and correctness of the computation results are confirmed with Haskind-Newman and energy conservation relations. In the present study, computations and analysis will be performed in beam wave case.

2. Solution Method

2.1 Mathematical Formulations

The present study is concerned with the development an optimal floating breakwater by optimizing the body shape. Therefore, in order to be able to analyze a model with arbitrary shape, the body shape is assumed to be asymmetric in all directions. The coordinate system adopted is shown in Fig. 1, where the body shape is arbitrary with respect to x, y and z-axes.

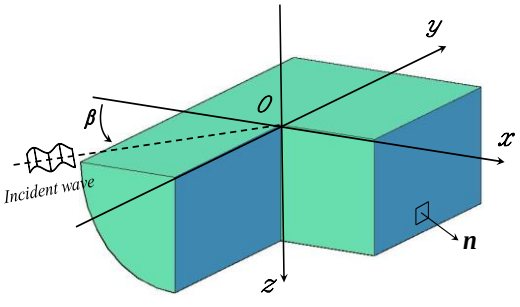

Fig. 1 Coordinate system and normal vector definitions

The origin of the coordinate system is placed at the center of the body and on the undisturbed free surface, and the z-axis is taken positive vertically downward. The water depth is assumed to be infinite. The regular wave is considered to be incoming with incident angle β with respect to the negative x-axis as shown in Fig. 1. Thus $\beta = -180$ deg. means the wave incoming from the positive x-axis which is considered in the present study.

Under the assumption of incompressible and inviscid flow with irrotational motion, the velocity potential can be introduced, satisfying Laplace's equation as the governing equation. The boundary conditions are linearized and all oscillatory quantities are assumed to be time-harmonic with circular frequency ω. Applying superposition principle, the velocity potential can be expressed as a summation of the incident-wave potential ϕ_0 and the disturbance potential ϕ as follows:

$$\Phi(x,y,z,t) = \mathrm{Re}\left[\left\{\phi_0(x,y,z) + \phi(x,y,z)\right\}e^{i\omega t}\right] \tag{1}$$

where ϕ_0 can be given explicitly as

$$\phi_0(x,y,z) = \frac{g\zeta_a}{i\omega} e^{-Kz - iK(x\cos\beta + y\sin\beta)} \tag{2}$$

with g the acceleration of gravity, ζ_a the amplitude of incident wave, and K the wave number given by $K = \omega^2 / g$. Furthermore the disturbance potential ϕ can be decomposed in the following form

$$\phi(x,y,z) = \frac{g\zeta_a}{i\omega}\left[\phi_7(x,y,z) - K\sum_{j=1}^{6}\frac{X_j}{\zeta_a}\phi_j(x,y,z)\right] \tag{3}$$

where ϕ_7 denotes the scattering potential in the diffraction problem, and ϕ_j is the radiation potential in the j-th mode of body motion with complex amplitude X_j. In 3D problems, we consider six degrees of freedom in general as shown in (3) which are surge $(j=1)$, sway $(j=2)$, heave $(j=3)$, roll $(j=4)$, pitch $(j=5)$, and yaw $(j=2)$. For the diffraction

problem, the sum of $\phi_0 + \phi_7$ is denoted as ϕ_D, which is referred to as the diffraction potential in this paper.

The governing equation and boundary conditions to be satisfied can be summarized as follows:

$$[L] \quad \nabla^2 \phi_j = 0 \qquad \text{for } z \geq 0 \tag{4}$$

$$[F] \quad \frac{\partial \phi_j}{\partial z} + K\phi_j = 0 \qquad \text{on } z = 0 \tag{5}$$

$$[H] \quad \frac{\partial \phi_j}{\partial n} = \begin{cases} n_j & (j = 1 \sim 6) \\ 0 & (j = D) \end{cases} \qquad \text{on } S_H \tag{6}$$

$$[B] \quad \frac{\partial \phi_j}{\partial z} = 0 \qquad \text{as } z \to \infty \tag{7}$$

and also an appropriate radiation condition of outgoing waves must be satisfied for $j = 1 \sim 7$. Here S_H denotes the body wetted surface and n_j the j-th component of the normal vector, defined as positive when directing out of the body and into the fluid.

By using Green's theorem, the governing differential equations of the present problem are turned into integral equations on the boundary. That boundary surface can be only the body surface S_H by introducing the free-surface Green function, and the resulting integral equations can be written in the form

$$C(P)\phi_j(P) + \iint_{S_H} \phi_j(Q) \frac{\partial}{\partial n_Q} G(P;Q)\, dS(Q) = \begin{cases} \iint_{S_H} n_j(Q) G(P;Q)\, dS(Q) & j = 1 \sim 6 \\ \phi_0(P) & j = D \end{cases} \tag{8}$$

where $C(P)$ is the solid angle, $P = (x, y, z)$ is the field point, $Q = (x', y', z')$ is the integration point on the body surface. $G(P;Q)$ is the free-surface Green function satisfying the linearized free-surface and radiation conditions, which can be expressed as

$$G(P;Q) = -\frac{1}{4\pi}\left(\frac{1}{r} + \frac{1}{r_1}\right) - \frac{K}{2\pi} G_W(R, z + z') \tag{9}$$

where

$$\left.\begin{matrix} r \\ r_1 \end{matrix}\right\} = \sqrt{(x - x')^2 + (y - y')^2 + (z \mp z')^2} \equiv \sqrt{R^2 + (z \mp z')^2} \tag{10}$$

$$G_W(R, z) = -\frac{2}{\pi}\int_0^\infty \frac{k \sin kz + K \cos kz}{k^2 + K^2} K_0(kR)\, dk - i\pi e^{-Kz} H_0^{(2)}(KR) \tag{11}$$

Here $K_0(kR)$ denotes the second kind of modified Bessel function of zero-th order and $H_0^{(2)}(KR)$ the second kind of Hankel function of zero-th order.

2.2 Higher-order Boundary Element Method

In order to attain high accuracy, the integral equation shown above was numerically solved by the Higher-Order Boundary Element Method (HOBEM), described in Kashiwagi [3]. The body surface is discretized into a number of quadrilateral panels. According to the concept of iso-parametric representation, both body surface and unknown velocity potential on each panel are represented with 9-point quadratic shape functions $N_k(\xi, \eta)$ $(k = 1 \sim 9)$ as follows:

$$\{x, y, z\}^T = \sum_{k=1}^{9} N_k(\xi, \eta) \{x_k, y_k, z_k\}^T \tag{12}$$

$$\phi(x, y, z) = \sum_{k=1}^{9} N_k(\xi, \eta) \phi_k \tag{13}$$

where (x_k, y_k, z_k) are local coordinates at 9-nodal points on a panel under consideration, and likewise ϕ_k denotes the value of the velocity potential (which is to be determined) at 9-nodal points of a panel.

The shape functions in (12) and (13) for a quadrilateral panel can be expressed in the form

$$\left.\begin{aligned} &N_k = \frac{1}{4}\xi(\xi + \xi_k)\eta(\eta + \eta_k) \quad \text{for } k = 1 \sim 4 \\ &N_5 = \frac{1}{2}\eta(\eta - 1)(1 - \xi^2), \quad N_6 = \frac{1}{2}\xi(\xi + 1)(1 - \eta^2) \\ &N_7 = \frac{1}{2}\eta(\eta + 1)(1 - \xi^2), \quad N_8 = \frac{1}{2}\xi(\xi - 1)(1 - \eta^2) \\ &N_9 = (1 - \xi^2)(1 - \eta^2) \end{aligned}\right\} \tag{14}$$

where index k denotes the local node number $(k = 1 \sim 9)$, as shown in Fig. 2.

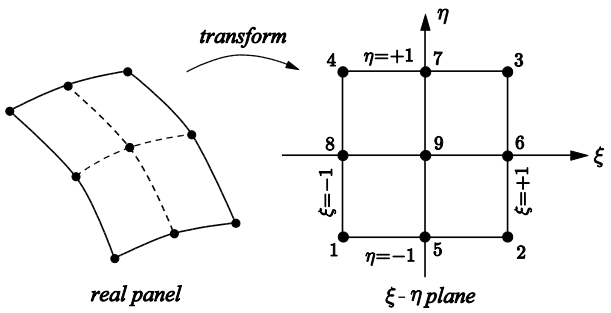

Fig. 2 Quadrilateral 9-node Lagrangian element

The normal vector on the body surface (each panel) can be computed with differentiation of the shape function as follows:

$$\boldsymbol{n}=\frac{\boldsymbol{a}\times\boldsymbol{b}}{|\boldsymbol{a}\times\boldsymbol{b}|},\ \boldsymbol{a}=\left(\frac{\partial x}{\partial\xi},\frac{\partial y}{\partial\xi},\frac{\partial z}{\partial\xi}\right),\ \boldsymbol{b}=\left(\frac{\partial x}{\partial\eta},\frac{\partial y}{\partial\eta},\frac{\partial z}{\partial\eta}\right) \quad (15)$$

Through a series of substitution, finally the boundary integral equations can be recast in a series of algebraic equations for the velocity potentials at nodal points consisting of panels. The results can be expressed in the form

$$C_m\phi_m+\sum_{\ell=1}^{NT}D_{m\ell}\phi_\ell=\begin{cases}\sum_{n=1}^{N}S_{mn}^{j} & j=1\sim 6\\ \phi_0(P_m) & m=1\sim NT\end{cases} \quad (16)$$

where

$$D_{m\ell}=\iint_{S_n}N_k(\xi,\eta)\frac{\partial G(P_m;Q)}{\partial n_Q}\left|J(\xi,\eta)\right|d\xi d\eta \quad (17)$$

$$S_{mn}^{j}=\iint_{S_n}n_j(Q)G(P_m;Q)\left|J(\xi,\eta)\right|d\xi d\eta \quad (18)$$

and index n denotes the serial n-th panel, index m the global serial number of nodal points, and $\ell=(n,k)$ is also the serial number of nodal points associated with (to be computed from) the k-th local node within the n-th panel. $|J(\xi,\eta)|$ in (17) and (18) denotes the Jacobian in the variable transformation. NT denotes the total number of nodal points and thus (16) is a linear system of simultaneous equations with dimension of $NT\times NT$ for the unknown velocity potentials at nodal points. The solid angle C_m in (16) is computed numerically by considering the equi-potential condition that a uniform potential applied over a closed domain produces no flux and thus zero normal velocities over the entire boundary.

The free-surface Green function, given by (11), can be computed efficiently by combining several expressions such as the power series, asymptotic expansions, and recursion formulae; its subroutine is available in Kashiwagi et al. [4].

2.3 Hydrodynamic Forces

Once the velocity potentials on the body surface are determined, it is straightforward to compute the hydrodynamic forces. The results are written in the form

$$F_{ij}=-\rho\iint_{S_H}\phi_j\,n_i\,dS\equiv A_{ij}-\frac{i}{\omega}B_{ij} \quad (19)$$

$$E_j=\rho g\zeta_a\iint_{S_H}\phi_D\,n_j\,dS \quad (20)$$

where F_{ij} is the radiation force in the i-th direction due to the j-th mode of motion and its real and imaginary parts are the added mass A_{ij} and damping coefficient B_{ij}. E_j in (20) denotes the wave-exciting force. These quantities are expressed with respect to the origin of the coordinate system shown in Fig. 1, and can be combined to obtain corresponding quantities expressed with respect to the center of gravity; which will be used in establishing the motion equations.

The equations of body motion with respect to the center of gravity can be established in a matrix form as follows:

$$\sum_{j=1}^{6}X_j^G\left\{-K\left(M_{ij}\,\delta_{ij}+F_{ij}^G\right)+C_{ij}^G\right\}=E_i^G\quad\text{for } i=1\sim 6 \quad (21)$$

Superscript G means quantities with respect to the center of gravity. M_{ij} denotes the generalized mass matrix, δ_{ij} is the Kroenecker's delta, and C_{ij}^G is the restoring-force coefficients due to the static pressure. By solving these coupled motion equations, the complex motion amplitude X_j^G can be determined and then the corresponding complex amplitude with respect

to the origin of the coordinate system X_j $(j=1\sim 6)$ can be obtained from

$$\left.\begin{aligned} X_j &= X_j^G + \varepsilon_{jkl}(x_G)_k X_{l+3}^G \\ X_{j+3} &= X_{j+3}^G \end{aligned}\right\} \quad (j=1\sim 3) \tag{22}$$

where ε_{jkl} denotes the alternating tensor for the outer product of vectors and $(x_G)_k$ $(k=1\sim 3)$ the ordinates of the center of gravity.

The numerical accuracy can be confirmed by checking the Haskind-Newman relation for the wave-exciting force and the energy-conservation relation for the damping coefficient. These relations are expressed as

$$E_j = \rho g \zeta_a H_j(K,\beta) \tag{23}$$

$$B_{ij} = \frac{\rho\omega K}{4\pi}\mathrm{Re}\int_0^{2\pi} H_i(K,\theta)H_j^*(K,\theta)\,d\theta \tag{24}$$

where $H_j(K,\theta)$ denotes the so-called Kochin function in the radiation problem, expressed as

$$H_j(K,\theta) = \iint_{S_H}\left(\frac{\partial\phi_j}{\partial n} - \phi_j\frac{\partial}{\partial n}\right)e^{-Kz-iK(x\cos\theta+y\sin\theta)}\,dS \tag{25}$$

2.4 Wave Elevation on Free Surface

The wave elevation on the free surface in the linear theory can be computed from

$$\frac{\zeta(x,y)}{\zeta_a} = \phi_0(x,y,0) + \phi_7(x,y,0) - K\sum_{j=1}^{6}\frac{X_j}{\zeta_a}\phi_j(x,y,0) \tag{26}$$

where the velocity potentials due to disturbance by a floating body can be computed from

$$\phi_7(P) = -\iint_{S_H}\phi_D(Q)\frac{\partial}{\partial n_Q}G(P;Q)\,dS(Q) \tag{27}$$

$$\phi_j(P) = \iint_{S_H}\left\{n_j(Q) - \phi_j\frac{\partial}{\partial n_Q}\right\}G(P;Q)\,dS(Q) \tag{28}$$

where $P=(x,y,0)$ is a point on the free surface.

In HOBEM, these velocity potentials can be computed by using the shape function and the solutions of the velocity potentials at nodal points. The integrals in (27) and (28) can be evaluated by summation over all panels, on which element computations can be done using the same scheme for the coefficients shown in Eqs. (17) and (18), with P placed on the free surface.

In this paper, we are concerned with the transmission and reflection waves by a floating breakwater. The transmission wave is defined by the wave in the lee side, propagating in the same direction as that of the incident wave. On the other hand, the reflection wave must be defined as the wave in the weather side, propagating to the opposite direction. Thus the incident-wave term $\phi_0(x,y,0)$ in Eq. (26) is subtracted from Eq. (26) in numerical computations for the reflection wave.

3. Results and Discussion

From the previous study conducted by Mahmuddin and Kashiwagi in [2], an optimal 2D shape had been obtained. Based on this shape, a 3D model is constructed by extruding it into longitudinal direction. The performance of the 3D model is found to be similar to the 2D one when the body dimension is quite long. The determined 2D shape and its dimension are shown in Fig. 3 and Table 1, respectively.

Table 1 also shows geometrical parameters which need to be assumed before computation which are center of gravity (*OG*) and roll gyrational radius (*Kzz*). The same values of these parameters are used in 3D model computations. The exact value of these parameters can only be known once the real model is constructed.

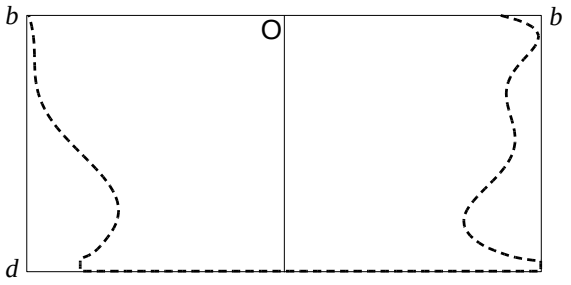

Fig. 3 Optimized 2D model shape

Tabel 1. Dimension of 2D model

Notations	Unit
Maximum breadth ($B=2b$)	2.0
Draft (d)	1.0
Center of gravity (OG)	0.82
Roll gyrational radius (Kzz)	0.614

The corresponding 3D model and dimension notations are shown in the Fig. 4 below. As it can be seen from the figure, the transverse sections of the model are uniform. The main goal of the present paper is to reduce the volume of the model by removing some portions of the uniform part without significantly reduced the performance of the original model.

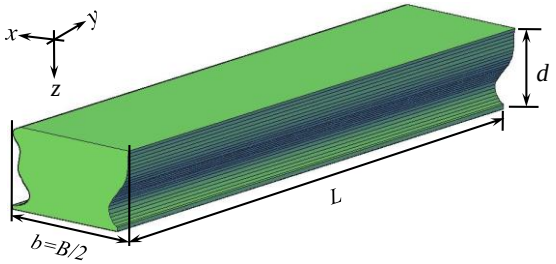

Fig. 4 Original 3D model shape

In 2D case, the wave reflection and transmission are easily defined because their magnitudes are same at any position of measurement. However, in 3D computations, the wave elevation will depend on the measurement position. Therefore, in order to fairly defined the wave transmission, 3 different positions along negative x-axis are defined for waves measurement which are at $-x/b$ = 4, 10 and 18 as illustrated in the figure below.

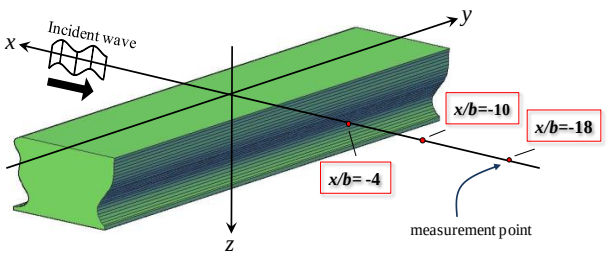

Fig. 5 Wave measurement positions

The performance of the optimized 2D model compared to original 3D model which has body length $L/b=40$, are found to be similar as shown in the figure below.

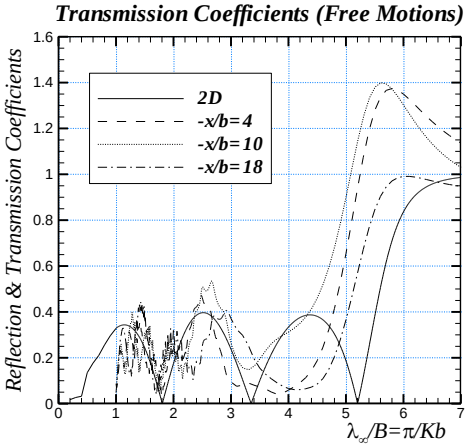

Fig. 6 Transmission coefficients of 2D and original 3D models

Because the original 3D model is considered to be less efficient in terms of technical and economical points of view, some modifications of the original 3D model are performed in this study. The first modification is performed by reducing the volume of the model in midst of the model. The modified model will be named as Model 1. The shape and dimension notations of Model 1 are shown in the following figure.

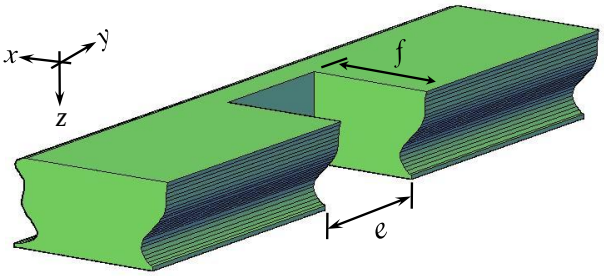

Fig. 7 Model 1

The main objective of modifications performed in this study is to reduce model volume with dimension $e/b=$ 10.667 and $f/b=1.6$. As shown in Fig. 1, the first modification or Model 1 removes the volume in midst of the model. The performance for this model is shown in following figure.

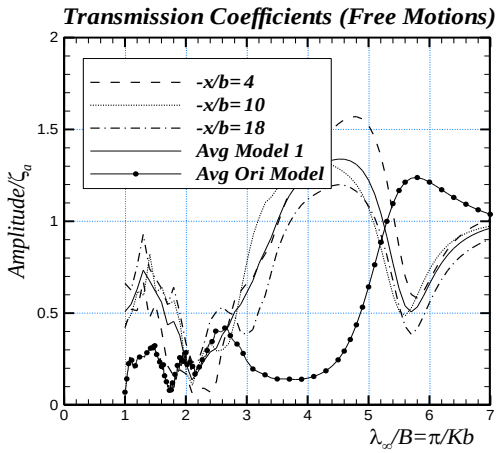

Fig. 8 Transmission coefficients of Model 1 and original model

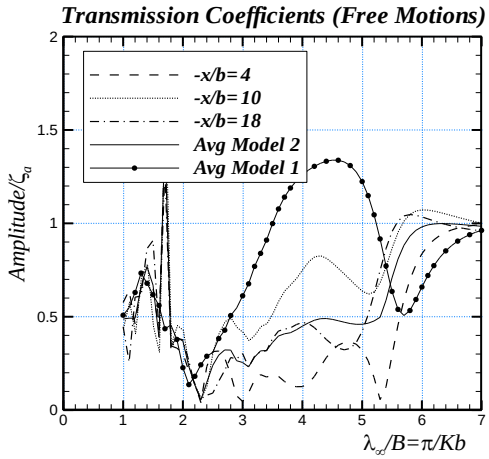

Fig. 10 Transmission coefficients of Model 1 and Model 2

In Fig. 8, besides the wave elevations measured in 3 defined positions, the average wave amplitude from these 3 wave amplitudes are also calculated and shown by a solid line. By comparing the transmitted waves of the original model and Model 1, it is obvious that the performance of the model is relatively poor. This performance reduction is caused by the shape change which is taken place at the same position with the wave measurement positions.

Therefore, the second modification named as Model 2 is performed by reducing the volume of the model in farther position from the center of the body. The removed part is also divided into 2 parts and placed near to each side of the body. The shape and dimension notations of the model are shown below.

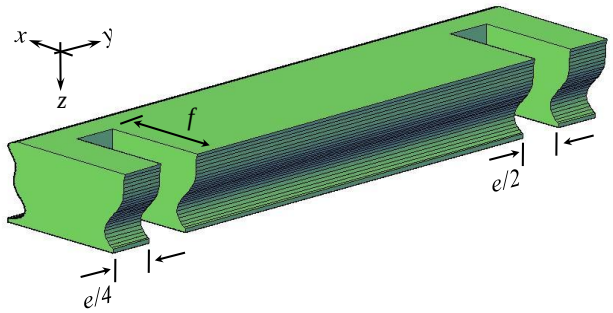

Fig. 9 Model 2

The computation results for Model 2 are shown below

As can be seen from Fig. 10, the model performance for this case is greatly improving compared to the previous model performance. However, a high peak in Fig. 10 can be noticed which is caused by the irregular frequencies. Same as the previous study in [2], an attempt to remove these frequencies are considered by placing some additional field points on the interior free surface of the body which is a method adopted by Haraguchi and Ohmatsu in [5]. However, this technique seems not effective on removing these frequencies. Therefore, other method should be implemented.

In order to obtain a more optimal performance model, the volume reduction is separated into several smaller parts so that the overall effect of modification can be minimalized. The shape and notations of the modified model for this case which is named as Model 3 are shown in the following figure.

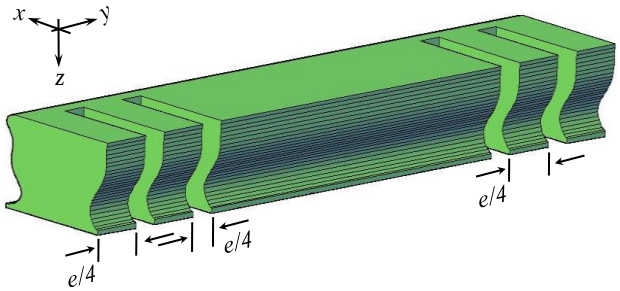

Fig. 11 Model 3

Computation results for model 3 compared to other models computation results are shown in the following figure.

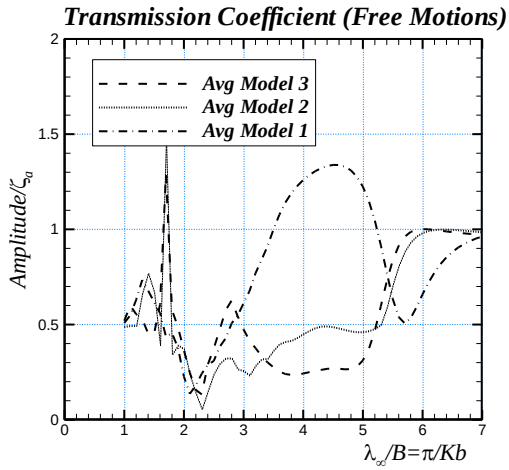

Fig. 12 Transmission coefficients of Model 1, 2 and 3

As shown in Fig. 12, the performance of Model 3 is much better than Model 2 and Model 1. This improvement can be obtained because of the distribution of modified shape into smaller parts. The distribution makes the overall effect to the performance to be smaller as well.

5. Conclusions

Based on an original which has an optimal performance, several models are constructed and computed in this study. Computation results show that a more realistic and efficient model for construction can be obtained by removing some parts of the model and dividing the removed section into smaller parts.

Acknowledgments

This research was carried out with support from Directorate General of Higher Education (DIKTI), Ministry of National Education using state university operational (BOPTN) fund of Hasanuddin University, Makassar.

References

[1] M. Kashiwagi, F. Mahmuddin, Numerical Analysis of a 3D Floating Breakwater performance, Proceeding of 22nd International Society of Offshore and Polar Engineers Conference (ISOPE), Vol. 3, No. 3 (2012) 1271-1278.

[2] F. Mahmuddin, M. Kashiwagi, Design Optimization of a 2D Asymmetric Floating Breakwater by Genetic Algorithm, Proceeding of 22nd International Society of Offshore and Polar Engineers Conference(ISOPE), Vol. 3, No. 3 (2012) 1263-1270.

[3] M. Kashiwagi, Bulletin Research Institute for Applied Mechanics, Kyushu University Japan, Vol. 170 (1995) 8-98.

[4] M. Kashiwagi, et. Al., 3D Boundary Element Method; Chapter – 5 Practical Hydrodynamics of Floating Bodies, Seizando Shoten, Co. Ltd, Vol. 1 (2003) 129-158.

[5] T. Haraguchi, S. Ohmatsu, On an Improved Solution of the Oscillation Problem on Non-wall sided Floating Bodies and a New Method for Eliminating the Irregular Frequencies, Transaction of West-Japan Society of Naval Architecture, No. 66, pp. 9 (1983)